JOURNAL OF MATERIALS SCIENCE 37 (2002) 603–613

Effect of particle size and surface treatment on constitutive properties of polyester-cenosphere composites

R. J. CARDOSO, A. SHUKLA*
Dynamic Photomechanics Laboratory, Department of Mechanical Engineering and Applied Mechanics, University of Rhode Island, Kingston, RI 02881, USA
E-mail: shuklaa@egr.uri.edu

A. BOSE
Department of Chemical Engineering, University of Rhode Island, Kingston, RI 02881, USA

Cenospheres (hollow, aluminum silicate spheres ranging from 10 to 400 μm in diameter) are used as filler in a homogeneous polyester composite. Particle size was varied to study its effect on mechanical properties of the composite. The effect of particulate surface modification using a silane coupling agent was also studied. Properties of the composites were characterized using standard testing methods. When compared to the largest particulate used, an increase in compression strength was achieved by particle size reduction and use of coupling agent. The Elastic modulus increased by using fine particles, while Poisson's ratio remained constant and independent of silane treatment or particle size. Fracture toughness increased with particle size reduction and increased further with silane surface modification. Dynamic compressive strength increased with particle size reduction, while silane did not show improvement. The addition of cenospheres as well as silane treatment increased the glass transition temperature for polyester. A given mass fraction of particulate, of a mean diameter D, will have the surface area between the particulate and matrix scale as D^{-1} (specific surface area). The sensitivity of these properties to cenosphere size is a direct function of the interfacial surface contacts between the polyester and the cenospheres and the specific surface area.

1. Introduction

An inexpensive, readily available byproduct of fly-ash from coal burning or heavy fuel oil combustion, called cenospheres [1–3], are used as the filler material in a polyester resin matrix to produce a macroscopically homogeneous particulate composite. Published cenosphere morphology and chemical composition indicates; spherical aluminum silicate micro spheres ranging from 10 to 400 microns in diameter, porous walls having a thickness of approximately 10% sphere diameter and bulk density of approximately 400 kg/m^3. Accuracy of the reported morphology and chemical composition was verified by the authors. Using cenospheres as filler can reduce the density of composite materials and structural members, while maintaining or increasing their strength, making these light-weight composites very desirable to the automotive, aircraft/aerospace industries. The use of cenospheres can also impact other mechanical, thermal and acoustic properties. Cenospheres are currently considered waste material and disposed of in landfills; therefore recycling is also a benefit. Fig. 1 shows SEM images of the 75–10 μm size range cenospheres before casting in polyester and clearly show the porous walls.

Cenospheres in aluminum matrix composites [4] and polymer matrices other than polyester [5, 6] have been studied in the past. Parameswaran and Shukla [7, 8] studied polyester-cenosphere composites cast as functionally gradient materials (FGMs). This study is exclusively on homogeneous polyester-cenosphere composites and focuses on the role of cenosphere size and surface properties on the mechanical properties of the composite. The composites were characterized by static tensile loading experiments (ASTM D638) [9], compressive experiments (ASTM D695) [10], and fracture toughness experiments (ASTM D5045) [11]. The dynamic mechanical behavior was characterized with the Split Hopkinson Pressure bar technique [12] and a dilatational wave speed measurement. In addition to the mechanical tests, a series of microscopic and thermal tests were conducted to analyze the microstructure of the composite, the surface composition of the

*Author to whom all correspondence should be addressed.

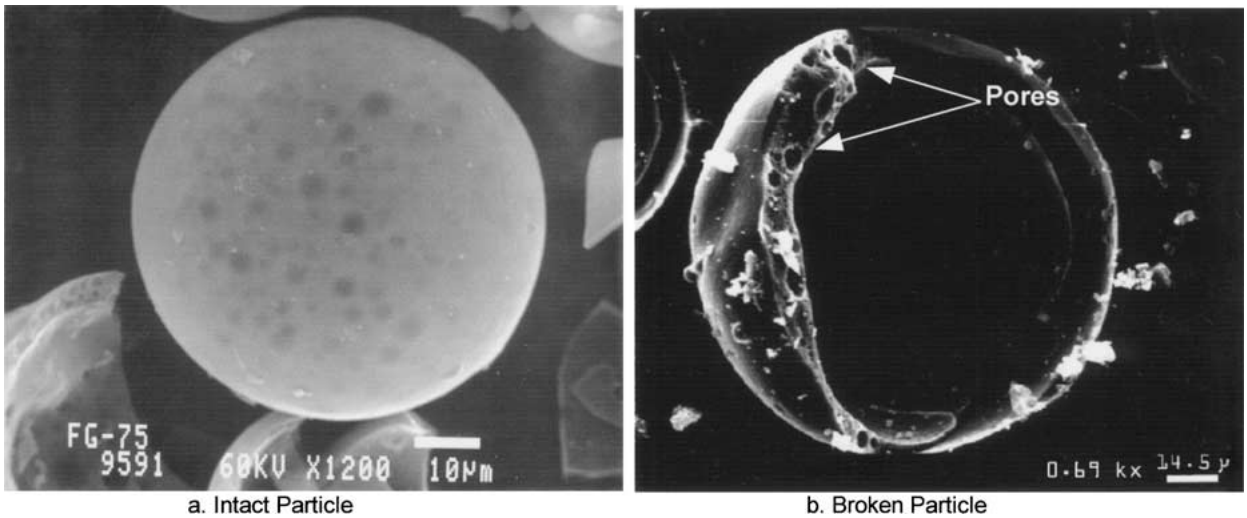

a. Intact Particle b. Broken Particle

Figure 1 SEM images of a cenosphere before casting in polyester, which clearly show the porous nature of the walls.

cenospheres and bonding of the silane-coupling agent to the cenospheres. Differential Scanning Calorimetry was used to measure changes in the glass transition temperature of the polyester. Scanning Electron Microscopy (SEM) and optical microscopy were used to examine the cenosphere's surface. Energy Dispersive Spectroscopy (EDS) and X-Ray Diffraction were used to identify cenosphere surface composition [13, 14].

2. Composite preparation, testing and characterization

2.1. Sieving

All cenospheres used in this study were purchased from Sphere Services Inc. TN, USA. All of the different particle size distributions in this study with the exception of the 75–10 range were sieved from the 300–10 grade with a standard mesh sieve column. The sieving was done on a mechanical shaker following standard soil testing procedures. The 300–10 grade and the 75–10 grade were purchased in that condition.

2.2. Composite casting

The composite was prepared using cenospheres in a polymeric matrix. The cenospheres have a low specific gravity (0.67) compared to that of polyester (1.18), therefore will migrate against the direction of gravity. This would result in a heterogeneous distribution of cenospheres in the matrix. In order to achieve a homogeneous composite, all castings were rotated about a horizontal axis at two revolutions per minute, drastically reducing the effective gravitational field inside the mold.

For a given mass fraction of cenospheres in a composite, the overall interfacial area between the inorganic silica-alumina surface and the polyester scales as D^{-1} (specific surface area), where "D" is the diameter of the cenospheres. Since a large proportion of failure in these materials is the result of cenosphere delamination, the particle size can be expected to influence a range of mechanical properties. In addition, modification of the interface to enhance the coupling between the polyester and cenosphere surface should also have significant effects on these mechanical properties. The experiments described in this paper are geared towards determining the effects of particle size on several mechanical properties of the composite. In addition to filler sizes, filler surface modifications were tested to study their effects on the properties of the composite. A silane coupling agent [Silquest A-174, Gamma-Methacryloxypropyltrimethoxy Silane, Witco Chemical Company] is coated onto the cenospheres to increase bonding between the polyester and the cenospheres. The silane group hydrolyses and bonds directly to the aluminum silicate cenosphere surface. The organic chain penetrates into the polyester matrix. This arrangement increases the bonding energy between the aluminum silicate and the surface of the polyester matrix. Ideally, only a monomolecular layer should be deposited, allowing the correct concentration of the organic chain.

The mold in which the sample was prepared in consisted of two sheets of acrylic having dimensions of 250 mm × 250 mm × 12 mm, a rib section was made using three pieces of aluminum bar stock screwed together to form a "U" shaped frame and a lid. Mylar sheets having thickness of 0.18 mm were cut to the same size as the acrylic sheets (250 mm × 250 mm) a small amount of glycerin was poured on the acrylic, the Mylar placed on top and the two were pressed together with a roller to remove all air bubbles. Silicone spray release agent was sprayed on the Mylar to aid in demolding and a thin bead of sensor safe silicone caulking was applied to both sides of the aluminum ribs to seal the mold. Mylar was used to aid in casting removal as well improve surface finish.

Polyester resin (MR-17090), manufactured by the Ashland Chemical Company is used as the matrix. In order for the matrix material to cure properly a catalyst (Methyl Ethyl Ketone Peroxide, 0.85% w/w) and an accelerator (Cobalt Octoate, 0.03% w/w) were used. The polyester resin was mixed thoroughly with the proper amounts of both catalyst and accelerator in that order. Cenospheres, 25% by weight of resin were slowly added to insure complete wetting as well as

avoid clumping. Once thoroughly mixed, the sample was placed in a 600 mm of Hg vacuum for 20 minutes to remove any trapped air bubbles. The mixture was then slowly poured into the mold and then sealed with the lid. Once sealed, the casting was cured rotating at 2 revolutions per minute for 48 hours at room temperature. After the 48-hour cure cycle, the mold was opened and the casting was post-cured in an air-circulating oven on a flat pane of glass, which was sprayed with mold release and coated with cenospheres to prevent sticking. The post-curing cycle was 4 hours at 52°C followed by 5 hours at 63°C. The post-curing at elevated temperatures ensures complete cross-linking of the polymer and yields the maximum possible stiffness and strength of the casting [7].

X-Ray diffraction of the polyester composite was used to learn more about the crystal structure of the polyester and the chemical identity of the cenospheres. The Bragg diffraction peaks for the cenospheres most closely matched aluminum silicate. The X-ray diffraction plot for polyester shown in Fig. 2, clearly illustrates the amorphous nature of the polyester.

2.3. Cenosphere surface treatment

Energy Dispersive Spectroscopy (EDS) yielded chemical composition values that matched Sphere Service's published literature, and is shown in Fig. 3. All EDS testing was done on a JEOL 1200 EX instrument in SEM mode, using a Noran Instruments detector, which used a Germanium crystal detector element and a light element (novar) window. A total of three tests were done on a 100-micron square at 3000X magnification and 20 kV in a low pulse processor rate. The results show 52% Oxygen, 23% Aluminum, 23% Silica and trace amounts of other elements.

The procedure for applying the silane coupling agent to the cenospheres was outlined in manufacturer literature. Special attention was needed in the solution mix due to the silane reacting with Silica, present in the beakers used. The Silane reacts with Silica only in the presence of water therefore two beakers were used to ensure separation of water and silane until the desired time. Also for optimum performance the pH of the solution had to be closely maintained between 4 and 5 and monitored continuously. The 290-gram sample of

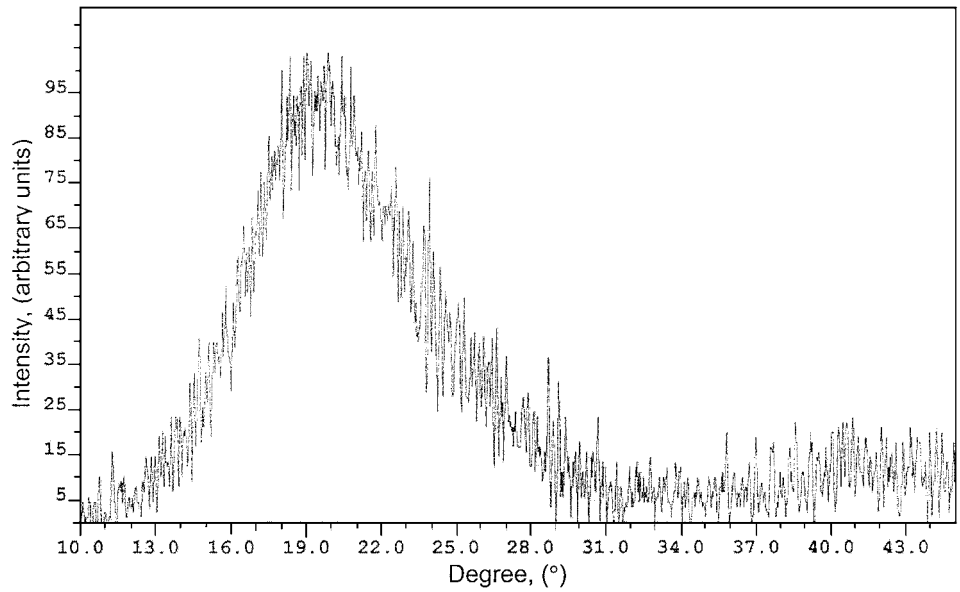

Figure 2 X-Ray diffraction trace plotting showing peak vs. angle for polyester sample which shows the amorphous nature of the polyester.

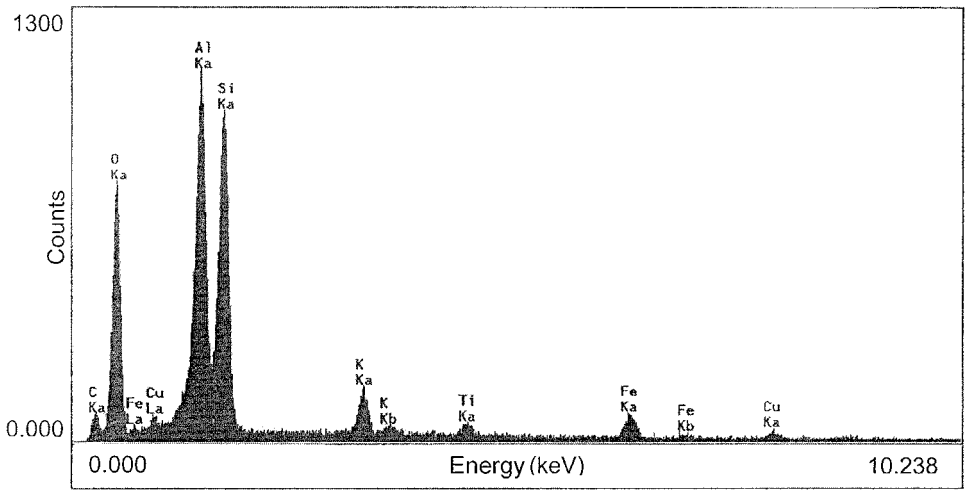

Figure 3 EDS trace showing elemental composition information of a cenosphere sample.

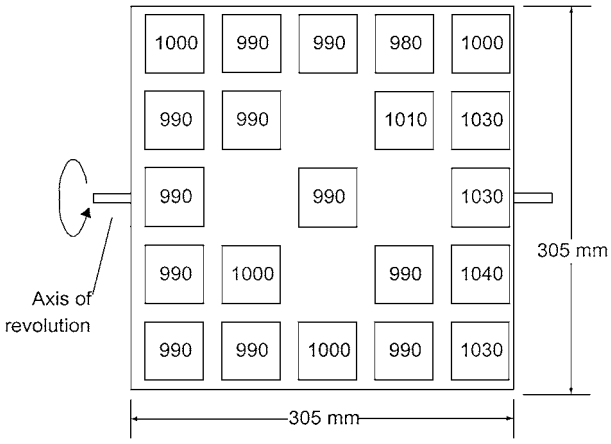

Figure 4 Density of casting at various locations in g/cc.

cenospheres required 0.029 grams of silane to produce one of the concentrations used (0.01%).

The sample was thoroughly mixed for 15 minutes. The still moist cenospheres were air dried for two hours at room temperature followed by drying in an air circulation oven at 80°C for an additional four hours. After the drying process clumping was observed, so sieving was done to ensure better surface wetting when mixed with polyester.

2.4. Physical properties

The density of the castings was measured at various locations as shown in Fig. 4. This was done to ensure that density did not vary significantly with position, which would indicate a non-homogeneous casting. By this method the casting technique was proven effective in consistently producing homogeneous sheets with no internal voids due to air being trapped at time of mold sealing.

2.5. Quasi-static elastic properties

2.5.1. Tensile experiments

Following ASTM standard D 638 [9] for rigid plastics, the initial portion of the tensile stress-strain curve was measured for the various filler grades tested. The specimen dimensions were chosen according to the ASTM specifications. Two 120 Ohm resistance strain gages from Micro-Measurements company type EA-06-250BG-120 were bonded to each specimen tested, one axially and one transversely. The testing was done on an Instron model 1125 tensile test machine using a 90 kN ("20,000 lb") load cell. A total of five repetitions were done for each experiment. The average values of Young's moduli and Poisson's ratios for all the filler size distributions used can be seen in Table I. The table lists filler grades in a range of their filler size (in microns) and is in order of decreasing mean diameter. (Note. S1 and S2 are different silane concentrations, 0.003% and 0.01% respectively). The "±" bands were calculated assuming normal distribution using the standard student's t [15] method with a 95% confidence. This confidence was done for all subsequent testing.

The Poisson's ratios remained essentially constant and independent of filler size used. As the data shows, addition of cenospheres reduces the Poisson's ratio when compared to virgin polyester. The relation between the lowering of Poisson's ratio by the addition of particulate closely follows the standard rule of mixtures. Using Poisson's ratio and volume fraction of cenospheres, 40% and 0.22 respectively, and the Poisson's ratio of polyester, 0.35; the calculated composite Poisson's ratio of 0.30 agrees well with measured values.

TABLE I Table displaying the results of elastic modulus and Poisson's ratio for the studied composites

Particulate size range (μm)	E (GPa)	Poisson's ratio ν
Polyester	3.98	0.35
300–180	4.16 +/− 0.10	0.29 +/−0.01
150–105	4.31 +/− 0.03	0.30 +/−0.01
105–10	4.33 +/− 0.02	0.30 +/−0.01
75–10	4.45 +/− 0.08	0.29 +/−0.01
75–10 S1	4.31 +/− 0.07	0.28 +/−0.01
75–10 S2	4.37 +/− 0.10	0.28 +/−0.01

When compared to virgin polyester, Young's modulus increases with the addition of cenospheres. The Young's modulus increased as the mean diameter decreased, indicating possibly better packing, or more uniform packing. Figs 5 and 6 shows data plots for a 75–10 composite for both engineering stress-strain and transverse strain versus axial strain respectively. The Young's modulus of the composite is a function of the Young's modulus of its constituents and their percent volume fraction by the Halpin Tsai relations, which has volume fraction as a variable. Since in this case volume fraction is held constant, the particle size becomes a modifier to the Halpin Tsai relations.

2.5.2. Compressive experiments

The quasi-static compressive strength of the composite was measured following ASTM standard D 695 [10]. The specimen chosen was a rectangular prismatic column having width and depth equal to one another and to half the height.

All compression specimens failed in shear, along a plane at 45° to the loading direction. The maximum compressive strength of the composites tested is given in Table II, which shows the filler grades used (size distribution in μm) and in order of decreasing numerical mean diameter.

The size effect trend is clearly seen where the compressive strength increases as the mean filler diameter decreases. The study of the crack surface indicates breakage of weak large cenospheres and pop out of finer ones. In the finer grade composites, the larger, weaker cenospheres are not present, so the compressive strength increases. Another possible reason may be that the projected cross-sectional area of the smaller cenospheres is larger than the large cenospheres. Having a larger area and being stronger, the compressive strength increases for the fine particulate composite.

2.6. Fracture toughness

The quasi-static fracture toughness of the composite was measured following ASTM standard 5045 [11] using the single edge notched specimen. A notch was cut into the specimen to simulate a crack. The crack was

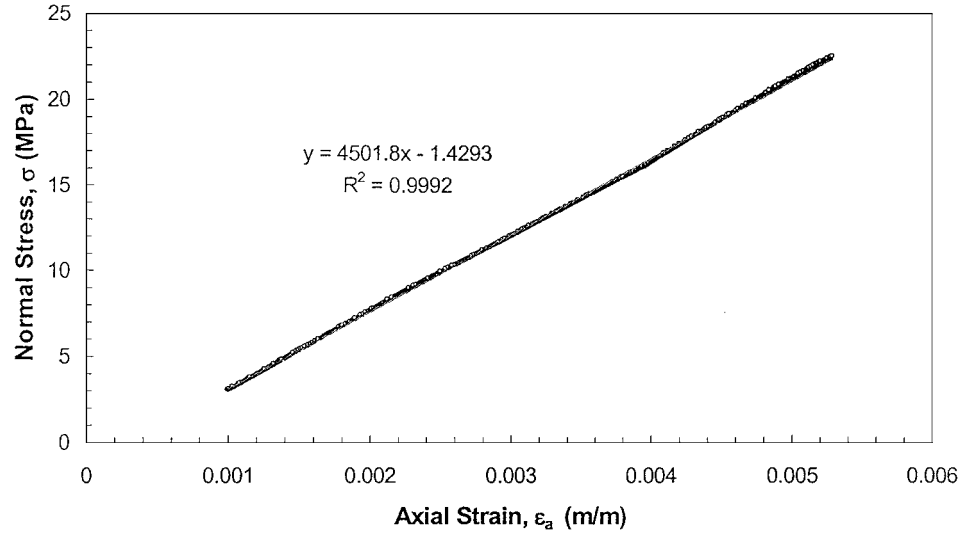

Figure 5 Plot of axial stress versus axial strain data with a curve fit to find the elastic modulus.

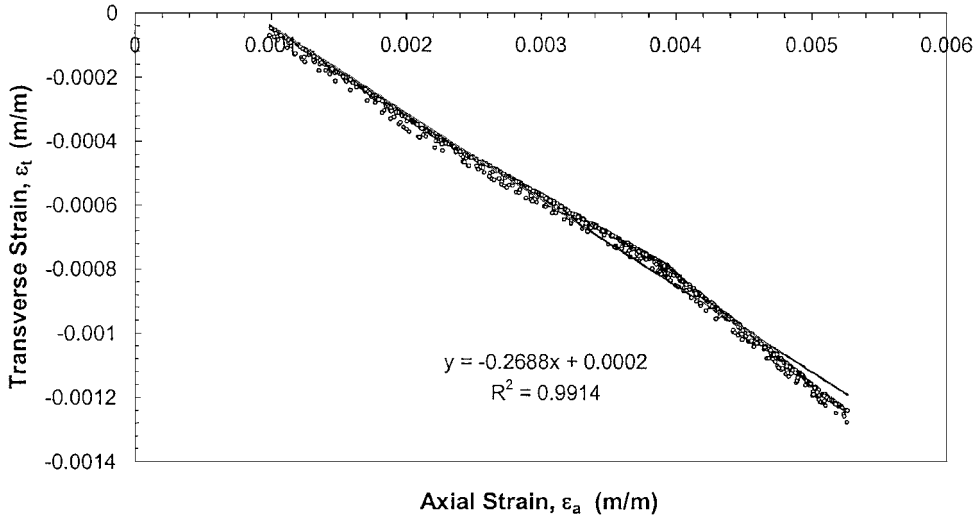

Figure 6 Plot of transverse strain versus axial strain data with a curve fit to find the Poisson's ratio.

TABLE II Table of compressive strengths of composites studied found under quasi-static loading condition

Particle size range (μm)	Compressive strength (MPa)
Polyester	155
300–180	104.0 +/−1.4
150–105	114.9 +/−1.3
105–10	115.8 +/−0.7
75–10	120.3 +/−0.9
75–10 S1	127.6 +/−0.5
75–10 S2	125.7 +/−1.0

TABLE III Table displaying results of fracture toughness experiments found with single edge notched 3 point bend test

Particle size range (μm)	K_{IC} (MPa$\sqrt{}$m)
Polyester	0.51
300–180	1.10 +/−0.02
150–105	1.35 +/−0.06
105–10	1.38 +/−0.09
75–10	1.45 +/−0.02
75–10 S1	1.52 +/−0.05
75–10 S2	1.38 +/−0.08

305 μm wide and was subsequently sharpened with a sharp razor blade, Fig. 7. The fracture toughness was calculated from Equation 1 using the failure load (F). The equation, which indicates the critical stress intensity factor for a plane-strain condition allows prediction of failure stress when a maximum flaw size in the material is known, or to determine maximum allowable flaw size when the stress is set.

$$K_I = \frac{FS}{BW^{3/2}} \frac{3\sqrt{x}\{1.99 - x(1-x)[2.15 - 3.93x + 2.7x^2]\}}{2(1+2x)(1-x)^{3/2}} \quad (1)$$

where a is the crack length, W is specimen thickness, B is specimen height, S is specimen length and $x = {}^{a}/_{W}$. All fracture testing was done on an Instron model 1125 test machine with the flexure test attachment and a 90 kN (20,000 lb). load cell. The only parameter recorded was the failure load.

The trend observed was that the fracture toughness increased 116% compared to virgin polyester with the addition of the large 300–180 μm cenospheres. The fracture toughness increased up to 185% as the mean filler diameter was decreased to the 75–10 μm range. The full results can be seen in Table III with the filler grade posted in decreasing mean diameter. A small

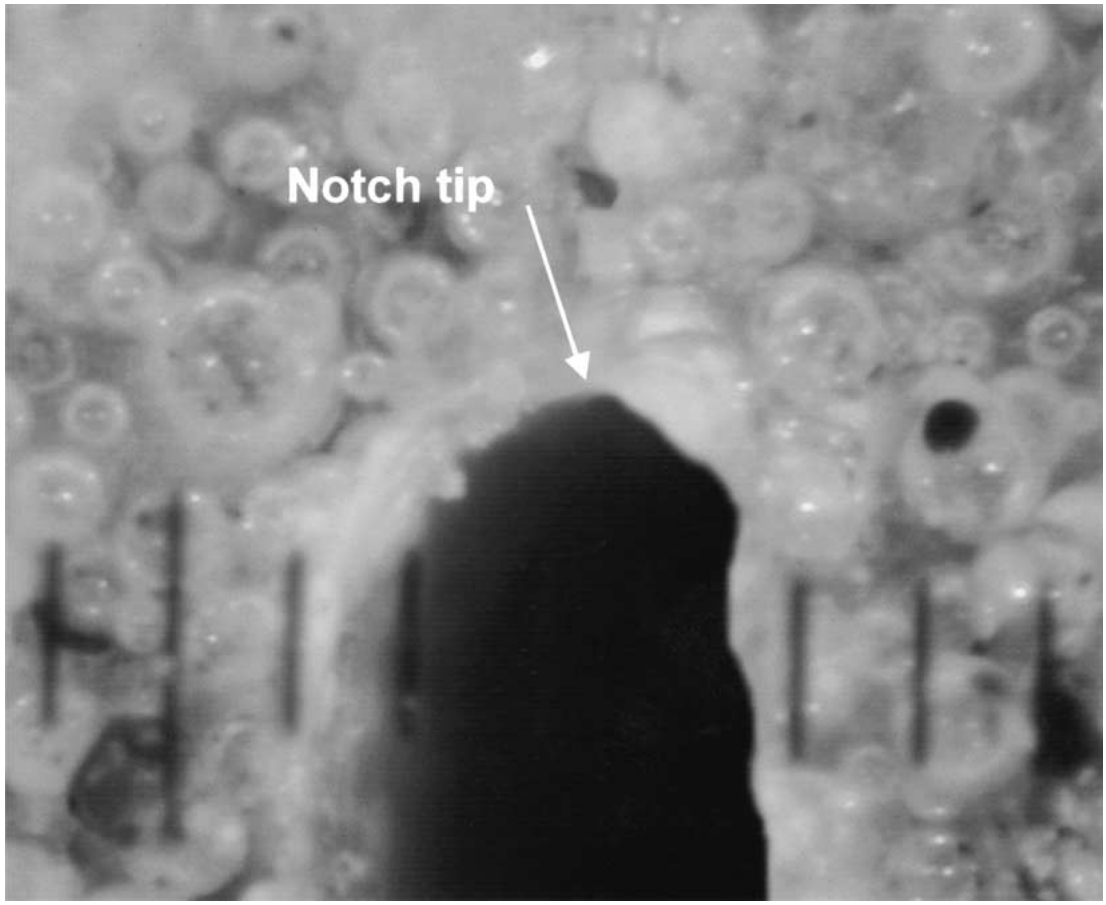

Figure 7 Image of notch cut into single edge notched specimen used in the three point bend experiments to determine fracture toughness. Space between scale marks is 100 μm.

increase of 5% was also observed between the untreated versus silane treated specimens. A possible explanation is that the addition of cenospheres increases the fracture toughness of the composite by blunting the crack. Also, since the fracture toughness of cenosphere material is higher than the matrix the fracture process zone develops through the matrix and around the cenospheres and this dissipates more energy, thereby increasing the fracture toughness. In the case of smaller filler, the area between matrix and filler is substantially increased while maintaining the weight fraction constant.

Fractographic analysis was done on the fracture surfaces of these specimens using a Nikon SMZ-U optical microscope. In the composites with the higher mean diameter filler, many broken large cenospheres were observed. This may be because larger cenospheres are more easily broken than the smaller ones. Figs 8 and 9 show the fracture surface of a fracture specimen. In Fig. 8 broken large cenospheres at the crack initiation region can be seen and are believed to be due to the cenosphere volume fraction being high enough that the cenospheres as well as the matrix share the load. In the case of the finer grade filler as well as the larger grades, step marks perpendicular to the crack surface were seen, indicating that the crack front is splitting into different planes and then rejoins to form a planar crack front. This was noted especially downstream of crack growth. Cenosphere pop out was much more evident than breaking in the finer filler composites.

TABLE IV Table displaying measured dilatational wave velocities for the various composites studied as well as comparing the calculated dynamic elastic modulus to the static elastic modulus for each

Particle range (μm)	Velocity (m/s)	Dynamic E (GPa)	Static E (GPa)	% Increase
300–180	2175 +/−20	4.33	4.16	4
150–105	2250 +/−30	4.61	4.31	7
105–10	2300 +/−20	4.81	4.33	11
75–10	2400 +/−25	5.28	4.45	19
75–10 S1	2420 +/−25	5.36	4.31	23
75–10 S2	2420 +/−30	5.36	4.37	25

2.7. Dynamic properties

The dilatational wave speed of the composite was calculated by measuring the arrival times of a compressive wave, which was initiated by a low velocity impact on a free edge of the composite plate. The waves were witnessed by two accelerometers a known distance apart. Fig. 10 shows the arrival times of two pulses. The voltage output accelerometers used were PCB model 303M37, mounted with wax 50.8 mm apart. A Tektronix model TDS-3014 oscilloscope was used to record the pulses. The striker was swung by hand with a small piece of plastic attached to the free surface of the casting to protect it from impact damage.

The collected dilatational wave speeds can be seen in Table IV. The dynamic modulus is calculated from Equation 2 using the given Poisson's ratio and

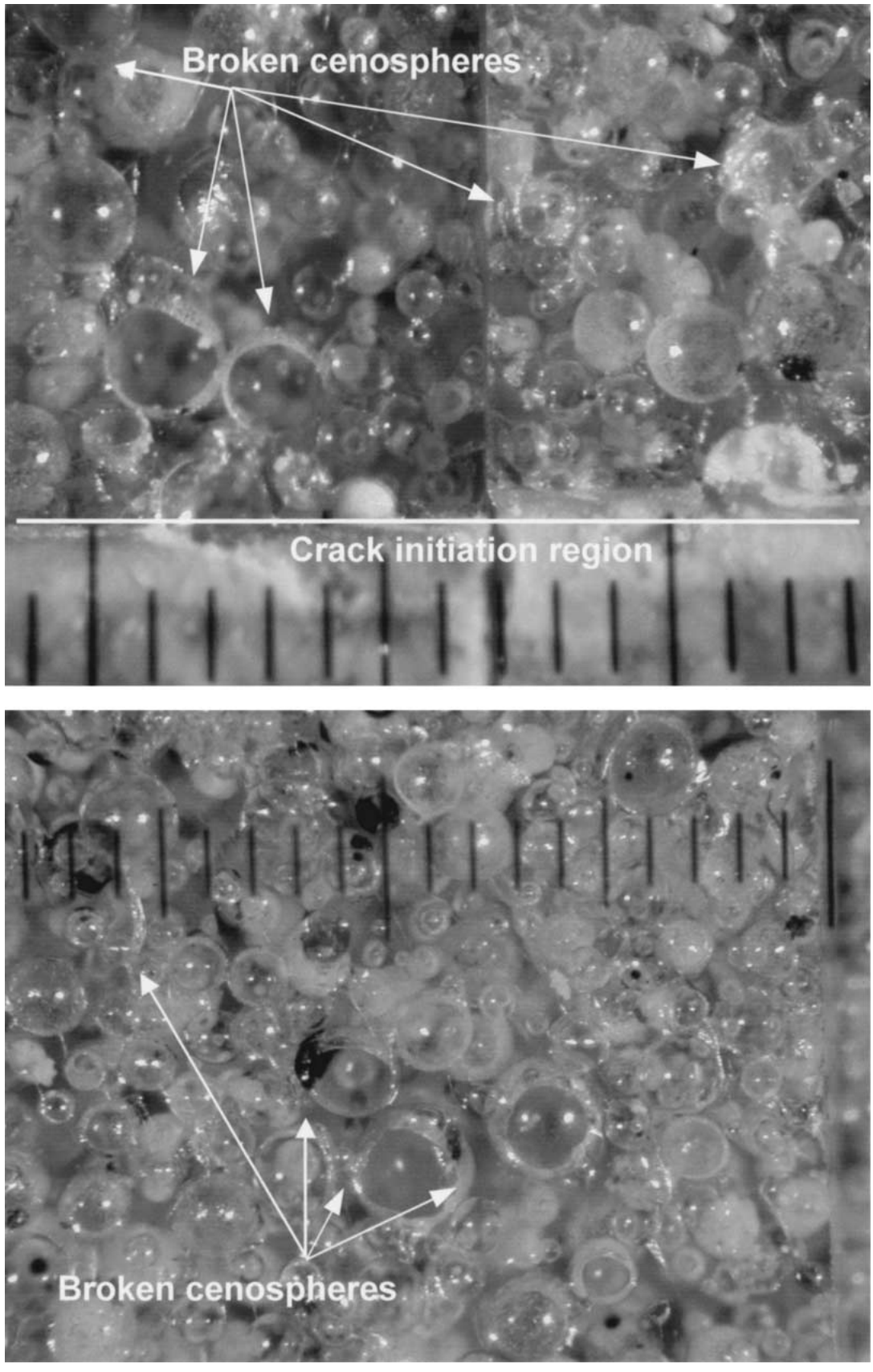

Figure 8 Fractograph of fracture surface of a fracture toughness experiment taken near the crack initiation zone. Space between scale marks is 100 μm.

density for each of the grades used and the measured dilatational wave speeds (C_L). The dynamic modulus appears to closely follow a trend similar to that of the static modulus except that it is much higher which is normally the case for all materials.

$$C_L = \sqrt{\frac{E}{(1-\upsilon^2)\rho}} \tag{2}$$

The dynamic stress-strain behavior of the material was also investigated using the Split Hopkinson

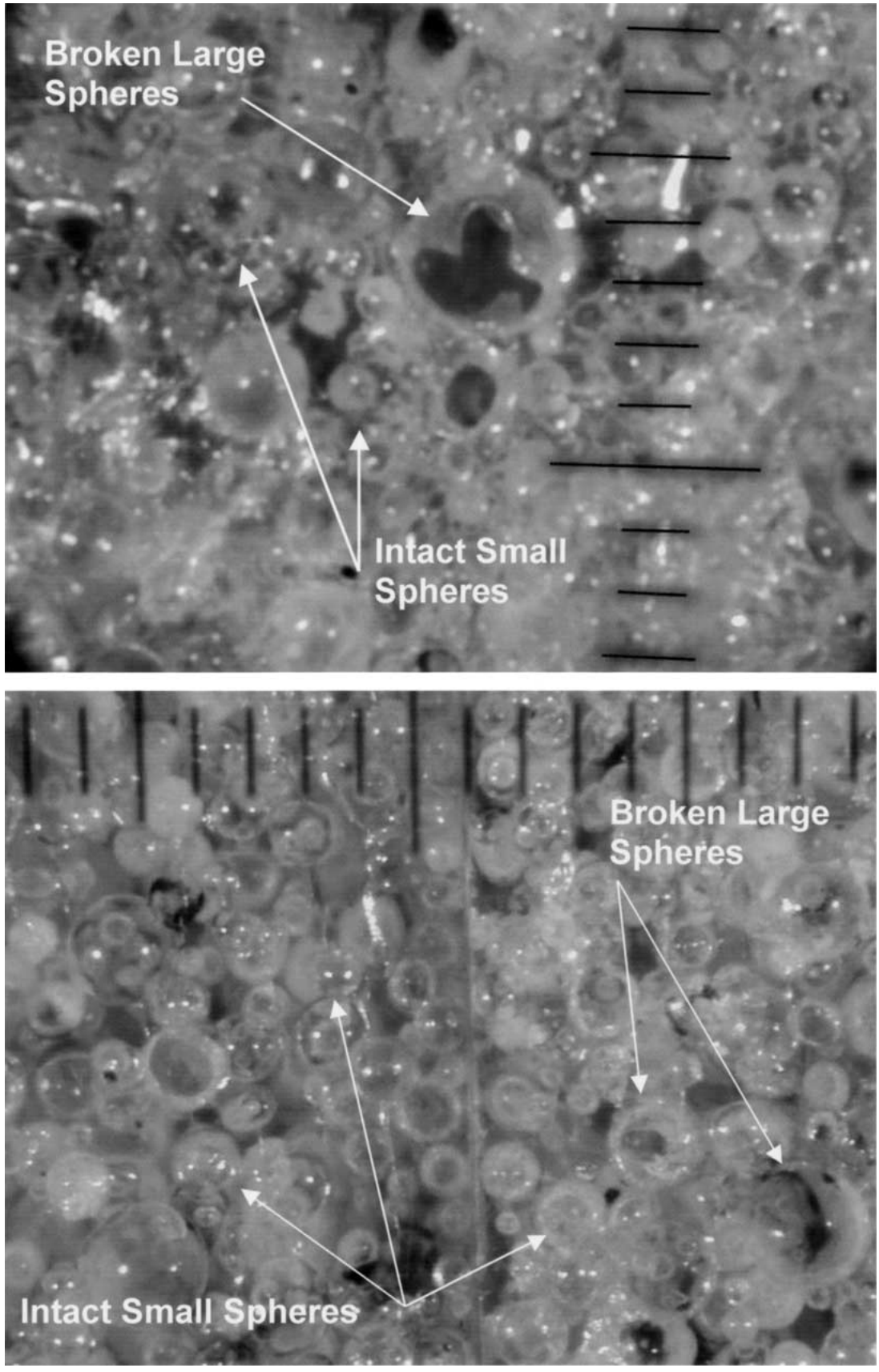

Figure 9 Fractograph showing surface of a fracture toughness experiment taken half way between the crack initiation zone and the top of the specimen. It is clearly seen that large cenospheres break while small ones either do not, or pop out. Space between scale marks is 100 μm.

Pressure Bar (SHPB) technique in compression [12]. The compressive SHPB setup consists of an incident bar and transmitter bar both of which are 12.7 mm ($^1/_2$ inch) diameter steel and instrumented with strain gages, see Fig. 11. The specimen is sandwiched between the incident bar and transmitter bar. The impact of a striker bar generates a compressive stress pulse of a finite length into the incident bar. Upon reaching the specimen some of the stress pulse gets reflected back as a tensile pulse and some gets transmitted through the specimen into

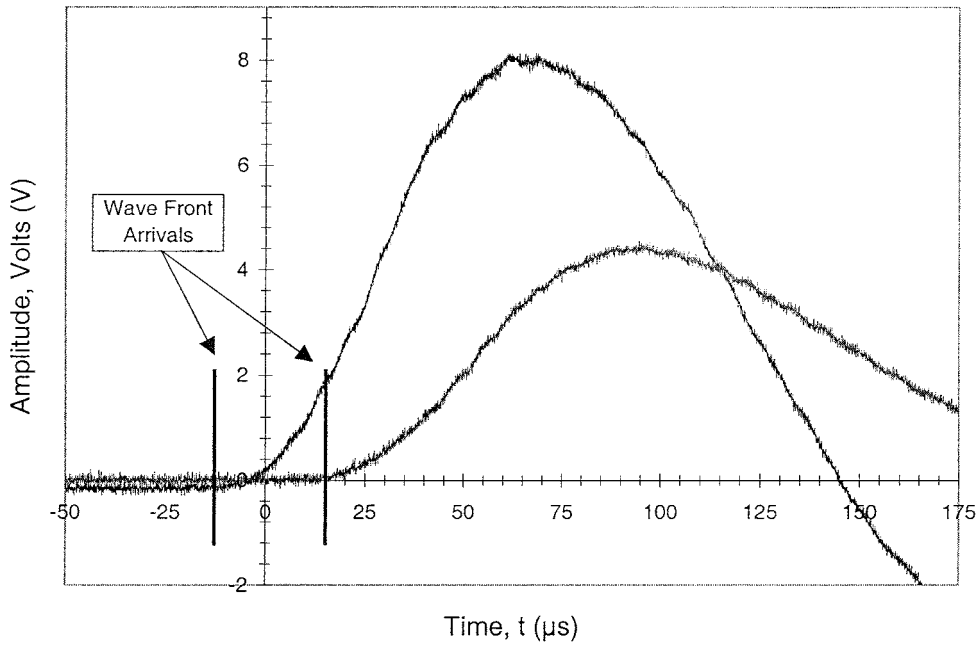

Figure 10 Plot showing output pulses from accelerometers used to find the arrival times at each and subsequently used to determine dilational wave velocity.

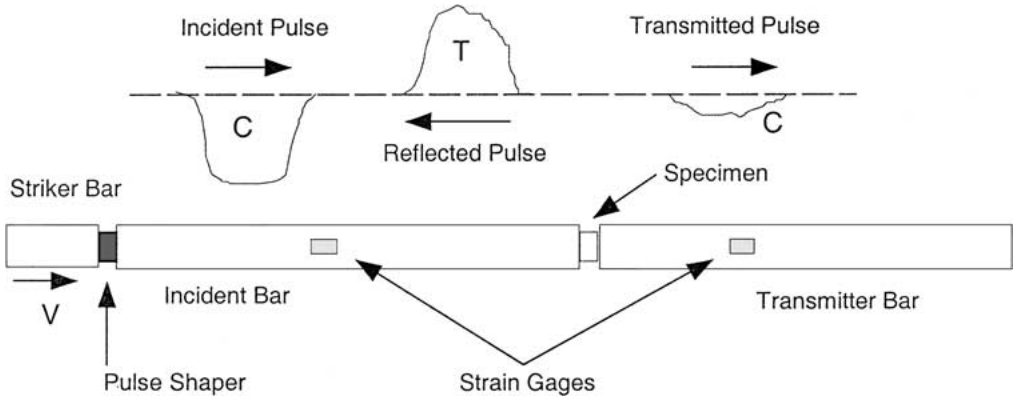

Figure 11 Schematic representation of the compressive SHPB setup used to conduct the dynamic compressive loading experiments.

the transmitter bar. The strain histories, which are time resolved are recorded and used for analysis by a LeCroy model 6810 data acquisition module.

The dynamic stress-strain response of the specimen can be obtained from the recorded strain histories using one dimensional wave propagation theory. Assuming a homogeneous specimen

$$\varepsilon_s(t) = \frac{-2c_b}{l_s}\int_0^t \varepsilon_r(t)\,dt$$

$$c_b = \sqrt{\frac{E_b}{\rho_b}}$$

$$\sigma_s(t) = E_b\frac{A_b}{A_s}\varepsilon_t(t) \qquad (3)$$

deformation the stress and strain (σ_s, ε_s) in the specimen can be generated as a function of time from the measured reflected and transmitted strains (ε_r, ε_t) using the relations shown in Equation 3. Where A_b and A_s are the cross-sectional areas of the bar and specimen respectively, l_s is the specimen length, c_b is the wave speed in the bar material and E_b and ρ_b are the Young's modulus and density of the bar material respectively. Cylindrical specimens with a diameter of 11 mm and thickness of 4 mm were used to obtain the dynamic stress strain profile of the composite.

The observed results were that the dynamic peak stress increased as mean filler diameter decreased very similar to the quasi-static compressive strength reported in a previous section. The values ranged from 155 MPa for the 300–180 composite to 178 MPa for the 75–10 composites. No significant difference was observed between the two silane treated batches and the untreated composite of the same grade. A typical result from the analysis of the SHPB data is shown in Fig. 12. Good equilibrium was observed for all experiments, (see lower right-hand "equilibrium", where the curve hovers at 1 and is the stress ratio on both faces of the specimen).

The SHPB testing was done with a 203.2 mm (8-inch) projectile fired at 207 kPa (30 psi). All specimens shattered into very small pieces. Upon closer examination

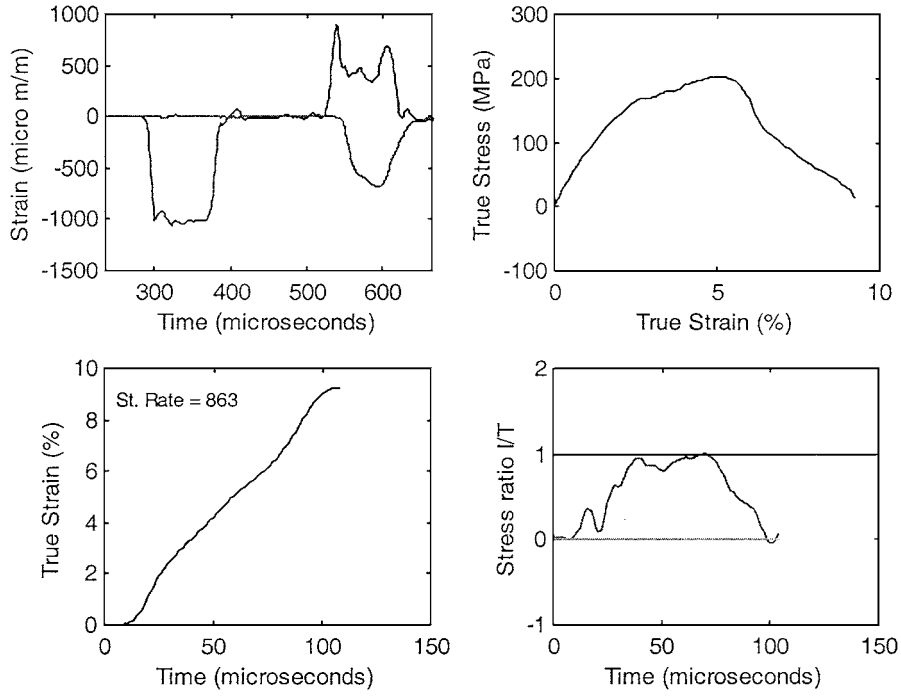

Figure 12 Results of analysis of SHPB strain histories used to find dynamic compressive strength of the composites.

TABLE V Table of SHPB experimental results showing the maximum dynamic peak stress for each of the studied composites

Particle size range (μm)	Dynamic compressive strength (MPa)
Polyester	265
300–180	154.0 +/−1.3
150–105	167.5 +/−1.4
105–10	174.5 +/−0.6
75–10	178.0 +/−1.0
75–10 S1	179.5 +/−0.6
75–10 S2	176.0 +/−0.8

it was observed that there was delamination between cenosphere and matrix and some, but very few broken cenospheres in the finer grade composites which were much more evident in the larger grade composites. Some matrix and cenosphere crushing was also observed in the finer debris collected from the larger grade specimens. Table V shows the measured values of dynamic compressive strength. The dynamic peak stresses are on average 50 MPa higher than the static peak stresses. The strain is applied dynamically; the stress builds faster than failure can relieve it, hence allowing higher dynamic stress.

2.8. Glass transition temperature

Differential Scanning Calorimetry was used to study the glass transition temperature to see the effects of the presence of cenospheres as well as silane surface treatments. This transition from solid to the glassy state is endothermic and appears as a minimum on the typical DSC plot. Our results show an increase in the glass transition temperature by 3°C for coated batch number 1 and 4°C for silane batch number 2.

The rise in the glass transition temperature is related to loss of mobility of the polymer chains located near the solid cenosphere surfaces. The coupling between the organic groups in the silane with the organic matrix further restrict the mobility of the polymer chains. This arrangement of polymer chains affects the local microstructure and thus the interfacial mechanical properties.

3. Conclusions

Addition of cenosphere particulate as fillers into a polyester matrix creates internal cenosphere-polyester interfaces. A range of mechanical properties of cenosphere-polyester composite are affected by particle size range used in the composite. These include elastic modulus increase of 7%, static compressive strength increase of 16%, dynamic compressive strength increase 16%, and fracture toughness increase of 32% compared to the largest particulate range used. When compared to virgin polyester, a 116% increase in fracture toughness was obtained by adding 300–180 μm filler, but a 185% increase was obtained by using untreated 75–10 filler. When silane treated 75–10 μm filler was used, a 200% increase in fracture toughness was achieved.

Coating of a silane coupling agent onto the cenospheres prior to their embedding within the polyester increases the interfacial strength, and allows several of the mechanical properties to improve. The incorporation of a controlled size, surface modified cenospheres into a polyester matrix is therefore a feasible route to producing lightweight, high strength polyester materials.

Acknowledgements

The authors extend acknowledgement to the National Science Foundation for their financial support under

grant number CMS-9900138. The authors also acknowledge the Ashland Chemical Company who very generously furnished all the polyester resin used in this study.

References

1. T. WANDELL, *The American Ceramic Bulletin* **75**(6) (1996) 79.
2. S. PERVEZ, G. S. PANDEY and V. K. JAIN, *Research and Industry* **38** (1993) 99.
3. R. M. CLAYTON and L. H. BACK, *Journal of Engineering for Gas Turbines and Power* **111** (1989) 679.
4. P. K. ROHATGI, R. Q. GUO, B. N. KESHAVARAM and D. GOLDEN, *Transactions of the American Foundrymen's Society* (103) (1995) 575.
5. E. E. BERRY, R. T. HEMMINGS and J. LEIDNER, *Plastics Compounding* **9**(7) (1986) 12.
6. N. CHAND, *J. Mater. Sci. Lett.* **7**(1) (1988) 36.
7. V. PARAMESWARAN and A. SHUKLA, *J. Mater. Sci.* **35** (2000) 1.
8. *Idem.*, *ibid.* **33** (1998) 3303.
9. American Society for Testing and Materials, "Standard test method for tensile properties of plastics," Annual Book of ASTM Standards, Designation D638-98 (1998).
10. American Society for Testing and Materials, "Standard test method for compressive properties of rigid plastics," Annual Book of ASTM Standards, Designation D695-96 (1996).
11. American Society for Testing and Materials, "Standard test methods for plane-strain fracture toughness and strain energy release rate of plastic materials," Annual Book of ASTM Standards, Designation D5045-99 (1999).
12. H. KOLSKY, "Stress Waves in Solids," Dover Publications, Inc. (New York, 1963).
13. S. P. KIM and S. C. KIM, *Polymer Engineering and Science* **31**(2) (1991) 110.
14. PÉREZ-CÁRDENAS, C. FERNANDO, DEL CASTILLO, FELIPE and VERA-GRAZIANO, RICARDO, *J. Appl. Polym. Sci.* **43** (1991) 779.
15. W. H. BEYER, "CRC Standard Mathematical Tables and Formulae" (CRC Press, Florida, 1991) p. 514.

Received 18 September 2000
and accepted 27 June 2001